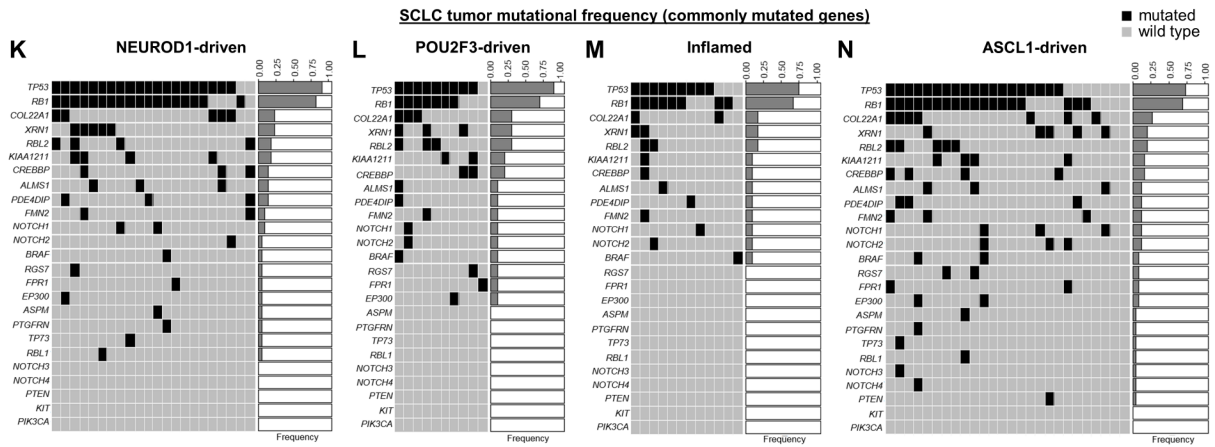
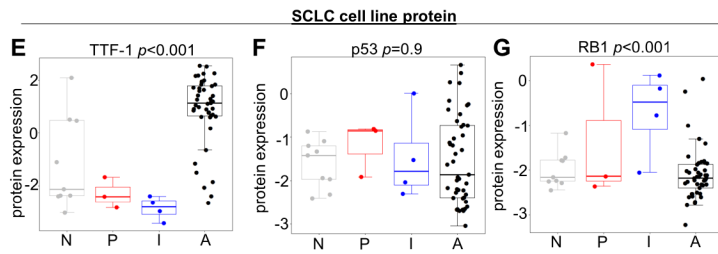
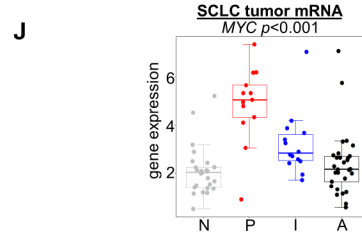
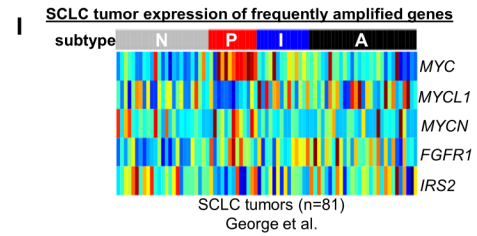
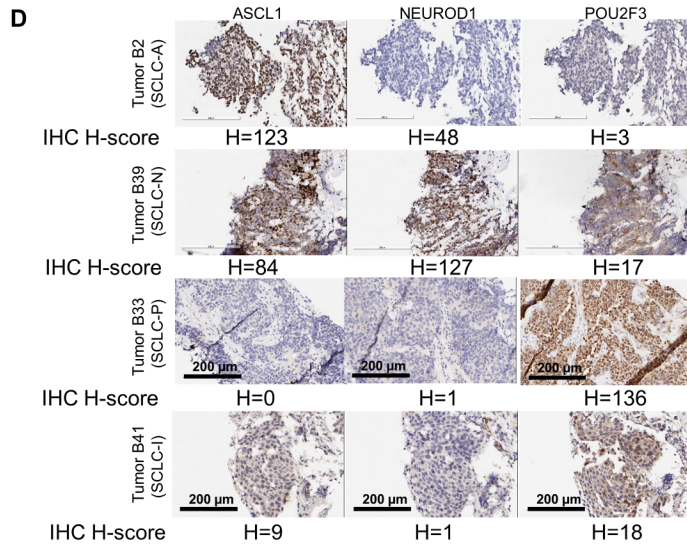
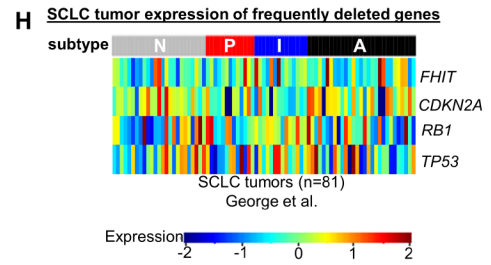
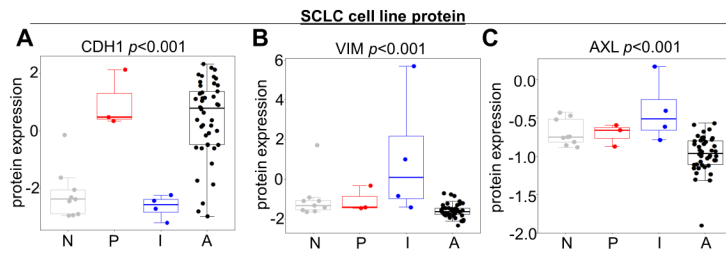
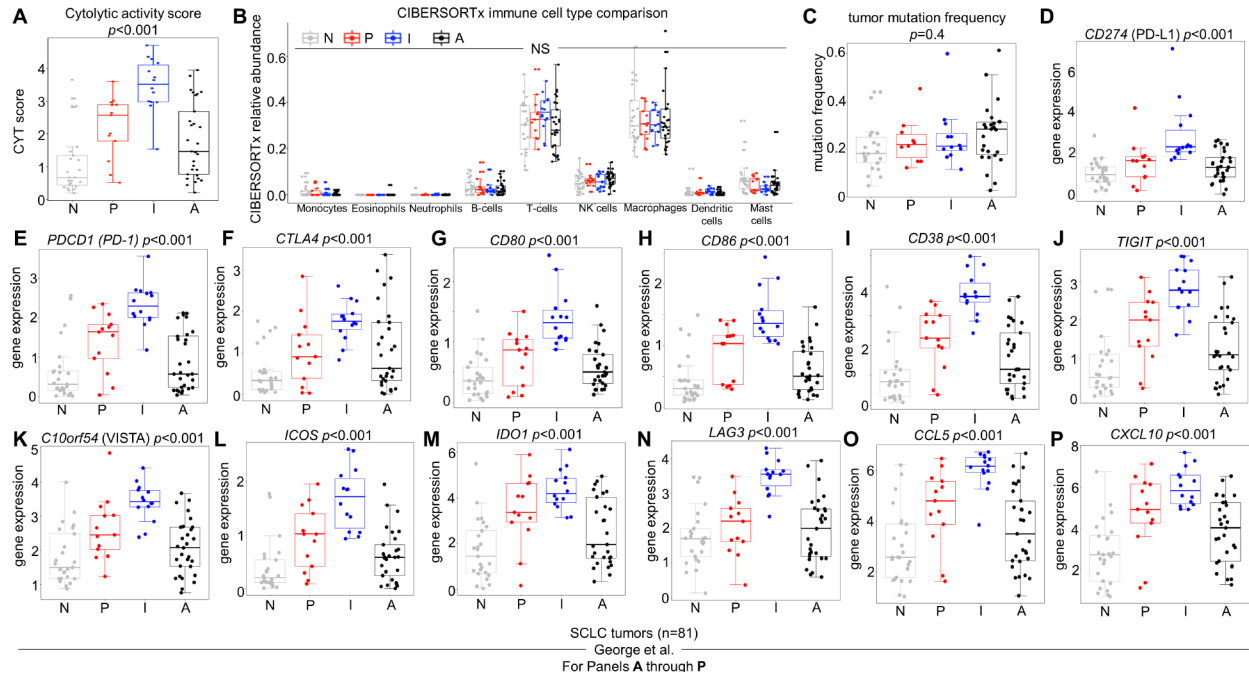


Supplementary Figure 1, related to Figure 1: NMF identifies four transcriptional subtypes of SCLC
 NMF consensus matrix illustrating consensus subtyping for 4 subtype version of clustering analysis (A). Differential expression NMF-identified genes (B) and, specifically, of *ASCL1*, *NEUROD1*, and *POU2F3*, across 3 subtype version of clustering analysis (C). Mean expression of *ASCL1*, *NEUROD1*, *POU2F3*, and *YAP1*, as well as differential expression of their transcriptional targets across SCLC tumor subtypes in George et al. dataset (D-H). Validation of four subtypes defined by gene expression of *ASCL1*, *NEUROD1*, *POU2F3*, or absence of all three in independent SCLC tumor (I) and SCLC cell line (J) cohorts. Sample sizes: n=81 tumors (A-H), n=23 tumors (I), and n=62 cell lines (J). Error bars: +/- 1.5x interquartile range (D-F, H). *p*-values are the result of one-way ANOVA (D-F, H).



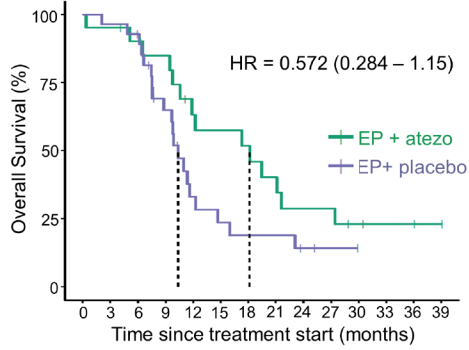
Supplementary Figure 2, related to Figure 2: Molecular and phenotypic distinctions between SCLC subtypes. Comparison of mean protein expression of the epithelial marker CDH1 (A) and mesenchymal markers VIM and AXL (B-C) across SCLC cell line subtypes. IHC demonstrating expression and associated H-score for ASCL1, NEUROD1, and POU2F3 in representative tumors from each SCLC subtype (D). Comparison of mean protein expression of lung tumor marker TTF1 (E), as well as p53 (F) and RB1 (G) across SCLC cell line subtypes. Differential gene expression of genes most commonly deleted in SCLC tumors across each subtype (H). Differential expression of genes most commonly amplified in SCLC tumors across each subtype (I). *MYC* gene expression across subtyped SCLC tumors (J). Using George et al. dataset, comparison of frequencies of mutations in 25 most frequently mutated in SCLC genes for tumors from each of the four subtypes (K-N). Sample sizes: n=59 cell lines (A-C, E-G), n=38 total tumor IHC assays (D), n=81 tumors (H-J), and n=60 tumors (K-N). Error bars: +/- 1.5x interquartile range (A-C, E-G, J). *p*-values are the result of one-way ANOVA (A-C, E-G, J-N).



Supplementary Figure 3, related to Figure 3: SCLC-I defines an inflamed subtype of SCLC.

Cytolytic activity (CYT) score (**A**) and CIBERSORTx relative immune cell populations (**B**) in George et al. Comparison of mean tumor mutation frequency (defined as ratio of mutated genes to total genes) across SCLC tumor subtypes in George et al. (**C**). Comparison of mean gene expression of various targetable immune checkpoints and their ligands (**D-N**), and STING-induced chemokines (**O-P**) across SCLC tumor subtypes from George et al. Sample size: n=81 tumors (**A-B, D-P**) and n=60 tumors (**C**). Error bars: +/- 1.5x interquartile range (**A-P**). p -values are the result of one-way ANOVA (**A-P**).

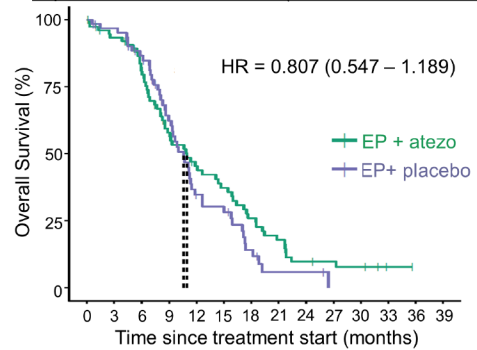
A IMpower133 Overall Survival (both arms SCLC-I only)



Number at risk

EP + atezo	21	20	18	16	11	10	9	7	5	5	3	2	2	1
EP+ placebo	28	27	25	15	7	5	4	4	2	1	0	0	0	0

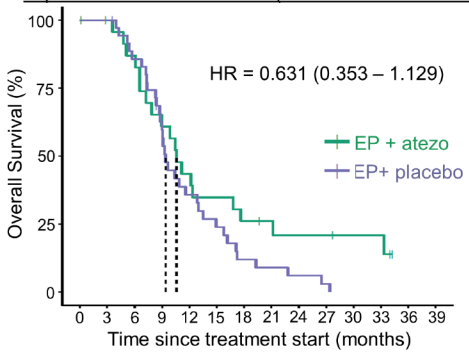
B IMpower133 Overall Survival (both arms SCLC-A only)



Number at risk

EP + atezo	77	69	58	38	28	23	16	11	6	5	4	1	0	0
EP+ placebo	63	59	49	32	16	13	6	2	2	0	0	0	0	0

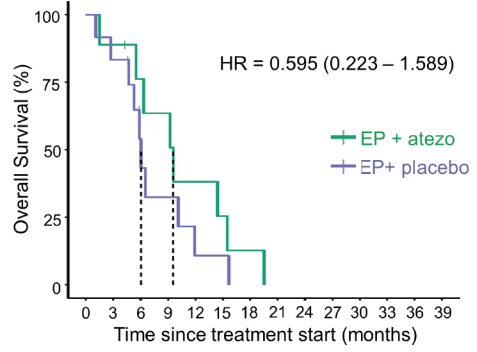
C IMpower133 Overall Survival (both arms SCLC-N only)



Number at risk

EP + atezo	25	23	20	14	10	8	6	5	4	4	3	3	0	0
EP+ placebo	36	36	30	20	12	8	4	3	2	1	0	0	0	0

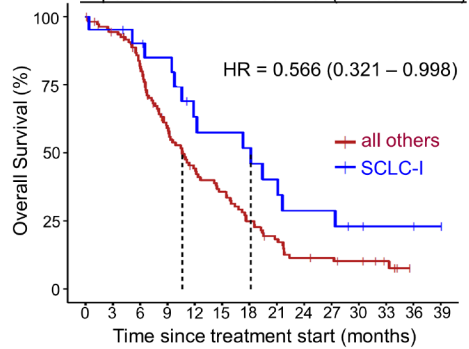
D IMpower133 Overall Survival (both arms SCLC-P only)



Number at risk

EP + atezo	9	8	6	5	3	2	1	0	0	0	0	0	0	0
EP+ placebo	12	10	5	3	1	1	0	0	0	0	0	0	0	0

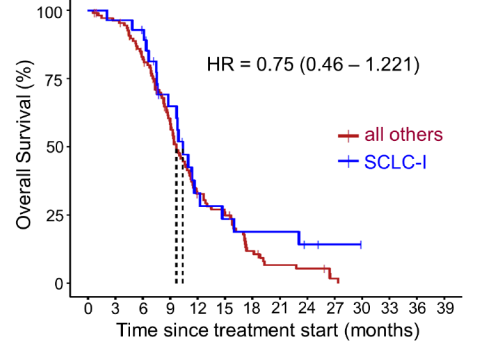
E IMpower133 Overall Survival (EP+atezo arm)



Number at risk

all others	111	100	84	57	41	33	23	16	10	9	7	4	0	0
SCLC-I	21	20	18	16	11	10	9	7	5	5	3	2	2	1

F IMpower133 Overall Survival (EP+placebo arm)

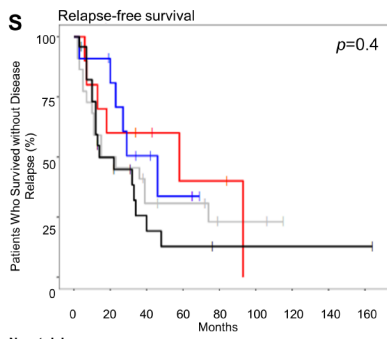
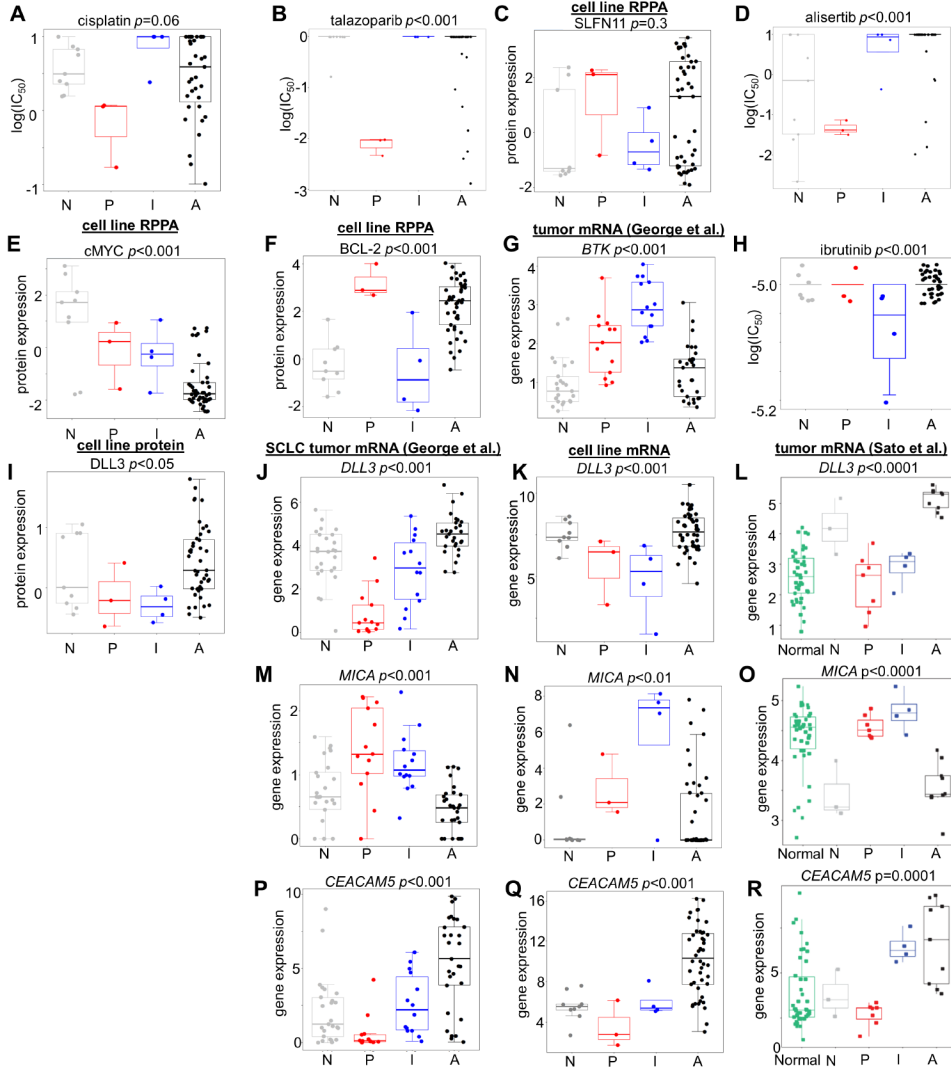


Number at risk

all others	111	105	84	55	29	22	10	5	4	1	0	0	0	0
SCLC-I	28	27	25	15	7	5	4	4	2	1	0	0	0	0

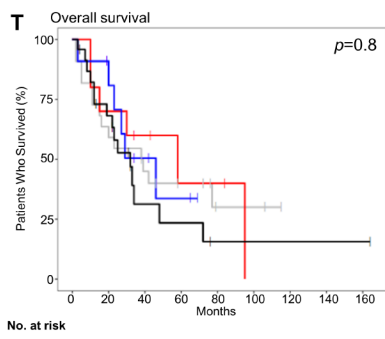
Supplementary Figure 4, related to Figure 3: SCLC-I defines an inflamed subtype of SCLC..

Kaplan-Meier curve comparing subtype-specific survival in EP+atezo vs EP+placebo arms in IMpower133 for SCLC-I (A), SCLC-A (B), SCLC-N (C), and SCLC-P (D). Kaplan-Meier curve comparing overall survival of SCLC-I patients to all other patients on the EP+atezo arm (E) and EP+placebo arm (F) of IMpower133. Sample sizes: n=49 patients (A), 140 patients (B), 61 patients (C), 21 patients (D), 132 patients (E), and 139 patients (F). Error bars: HR includes 95% CI range.



No. at risk

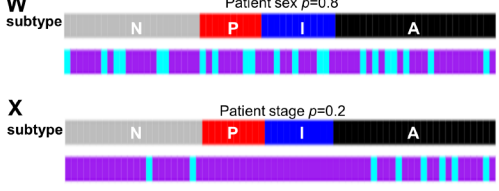
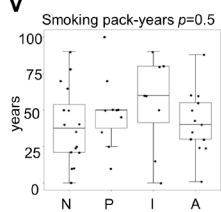
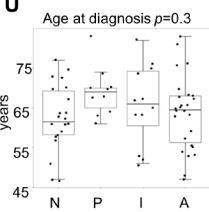
N (n=22)	22	11	6	5	2	2	0	0	0
P (n=10)	10	6	5	2	2	0	0	0	0
I (n=11)	11	9	4	2	0	0	0	0	0
A (n=24)	24	10	4	2	1	1	1	1	1



No. at risk

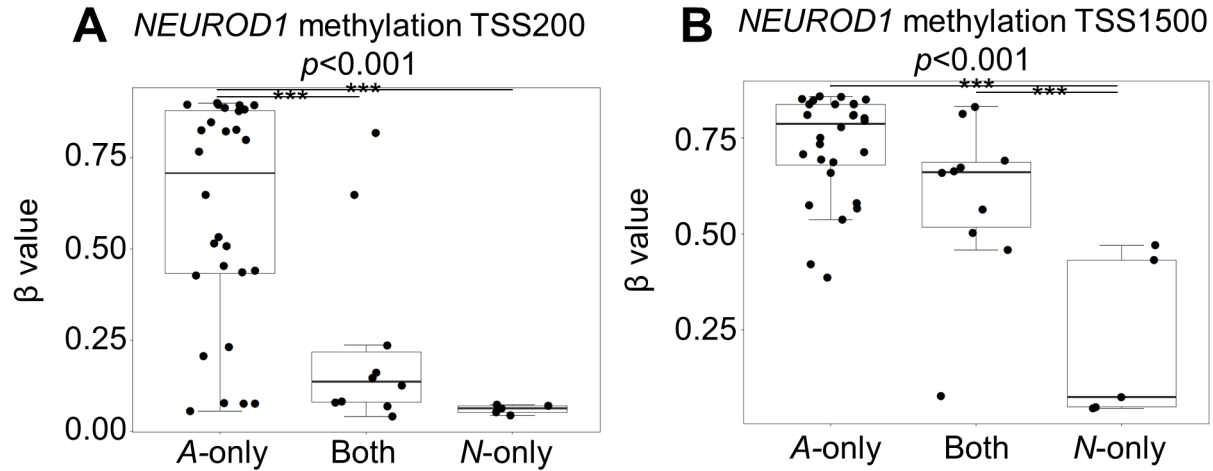
N (n=22)	22	11	6	5	2	2	0	0	0
P (n=10)	10	6	5	2	2	0	0	0	0
I (n=11)	11	9	4	2	0	0	0	0	0
A (n=24)	24	10	4	2	1	1	1	1	1

■ *NEUROD1*-driven (N)
■ *POU2F3*-driven (P)
■ Inflamed (I)
■ *ASCL1*-driven (A)

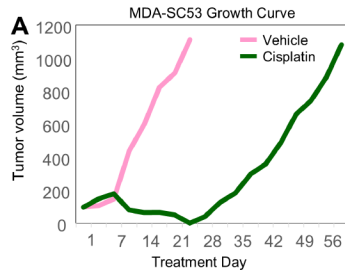


■ female
■ male
■ ES
■ LS

Supplementary Figure 5, related to Figure 4: SCLC subtypes possess unique therapeutic vulnerabilities. Comparison of mean IC_{50} values for *in vitro* treatment with cisplatin of SCLC cell lines from each subtype (**A**). Representative example of *in vitro* response to a PARPi (talazoparib, **B**). Comparison of mean protein expression of SLFN11 (**C**) among cell lines from each subtype. Representative example of *in vitro* response to an AURKi (alisertib, **D**). Comparison of mean protein expression of predictive biomarkers including cMYC and BCL2 (**E-F**) among SCLC cell lines. Expression of *BTK* gene among tumors of each subtype (**G**) and mean IC_{50} values between subtypes for the BTK inhibitor ibrutinib (**H**). Differential mean expression of DLL3 protein among SCLC cell lines (**I**). Differential mean gene expression (**J-L**) among subtypes for *DLL3* in tumor and cell lines data sets. Differential mean expression between subtypes of genes encoding targets of established antibody-based therapies including *MICA* (**M-O**), and *CEACAM5* (**P-R**). Kaplan-Meier curves illustrating relapse-free (**S**) and overall survival (**T**) for patients with tumors of each subtype from George et al. Comparison of mean age at diagnosis (**U**) and smoking pack-years (**V**) for patients with tumors of each subtype. Comparison of fraction of male/female (**W**) and extensive-stage/limited-stage (**X**) for each subtype. *p*-values are the result of one-way ANOVA (**A-R**, **U-V**). Sample sizes: n=62 cell lines (**A-B**, **D**, **H**, **K**, **N**, **Q**), 59 cell lines (**C**, **E-F**, **I**), 81 tumors (**G**, **J**, **M**, **P**), 23 tumors (**L**, **O**, **R**), and 67 patients (**S-X**). Error bars: +/- 1.5x interquartile range (**A-R**, **U-V**). Log rank test was used to compare the Kaplan-Meier RFS and OS curves (**S-T**), one-way ANOVA was used to calculate *p*-value in **C-D**, and Fisher's exact test was used to compute the association between categorical clinical variables (**W-X**).

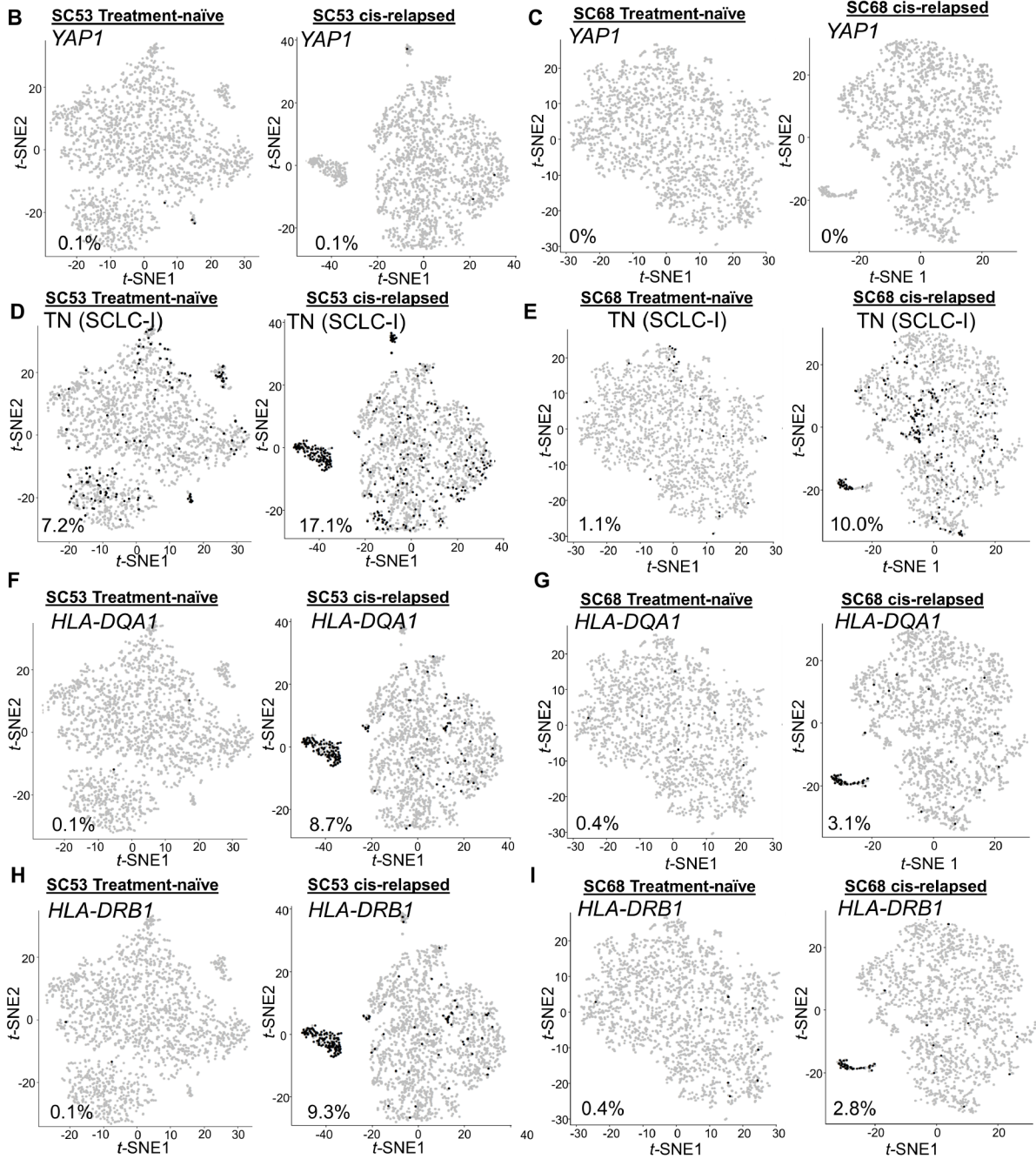


Supplementary Figure 6, related to Figure 5: Intratumoral heterogeneity of SCLC subtypes in tumors and tumor-derived models. Mean methylation beta-values of promoter region of *NEUROD1* gene within 200 nucleotides (A) or 1500 nucleotides (B) from transcriptional start site (TSS) for cell lines classified as *ASCL1*-only (A-only), *NEUROD1*-only (N-only), or both. Sample sizes: n=43 cell lines (A-B). p -values were calculated using two-sided unpaired T-test (A-B). Error bars: ± 1.5 interquartile range (A-B).

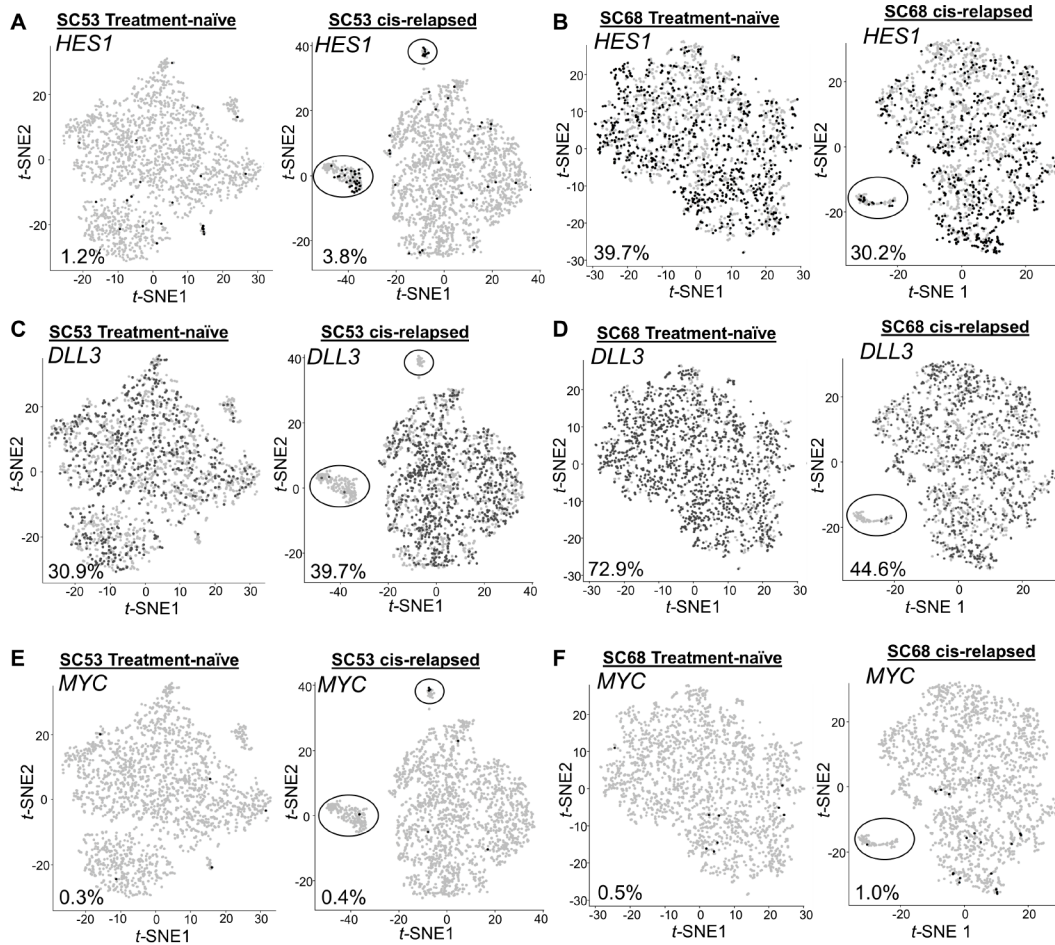


Gene Expression Detected

● NO
● YES

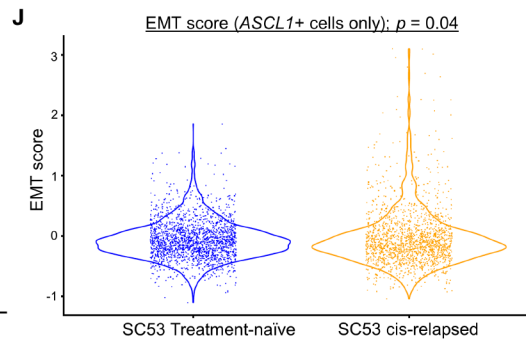
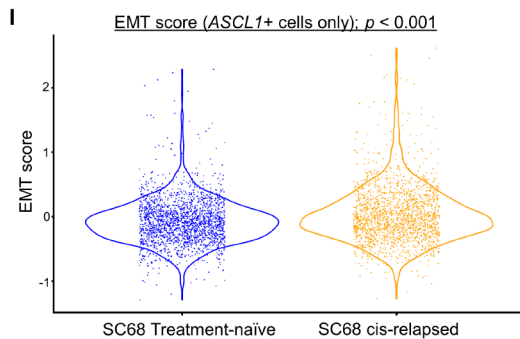
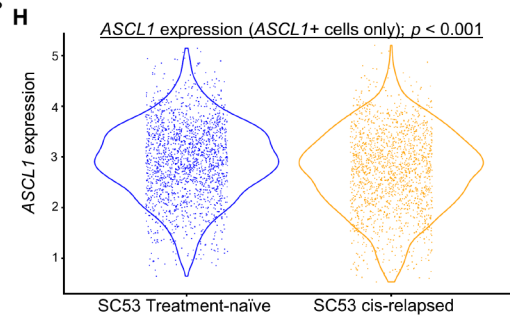
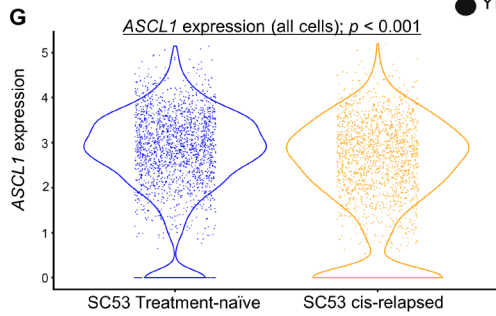


Supplementary Figure 7, related to Figure 6: Emergence of SCLC-I populations coincides with cisplatin resistance in SCLC-A predominant xenograft models. Curves illustrating tumor growth in MDA-SC53 treated with vehicle (pink, n=3) or cisplatin (green, n=3), including subsequent growth following relapse and platinum resistance, prior to collection for single-cell RNAseq experiments. Similar curve for MDA-SC68 previously reported (Stewart et al., 2020b). t-SNE feature plots from scRNAseq for *YAP1* comparing parental, treatment-naive and cisplatin-resistant/relapsed (cis-relapsed) CDX models (MDA-SC53, **B**; MDA-SC68, **C**). t-SNE feature plots from scRNAseq for triple-negative (TN)/SCLC-I cells, which lack *ASCL1*, *NEUROD1*, and *POU2F3* (MDA-SC53, **D**; MDA-SC68, **E**). t-SNE feature plots from scRNAseq for *HLA-DQA1* (MDA-SC53, **F**; MDA-SC68, **G**) and *HLA-DRB1* (MDA-SC53, **H**; MDA-SC68, **I**). Sample sizes: n=3 mouse tumors per arm (**A**), n=2000 cells (**B-I**).

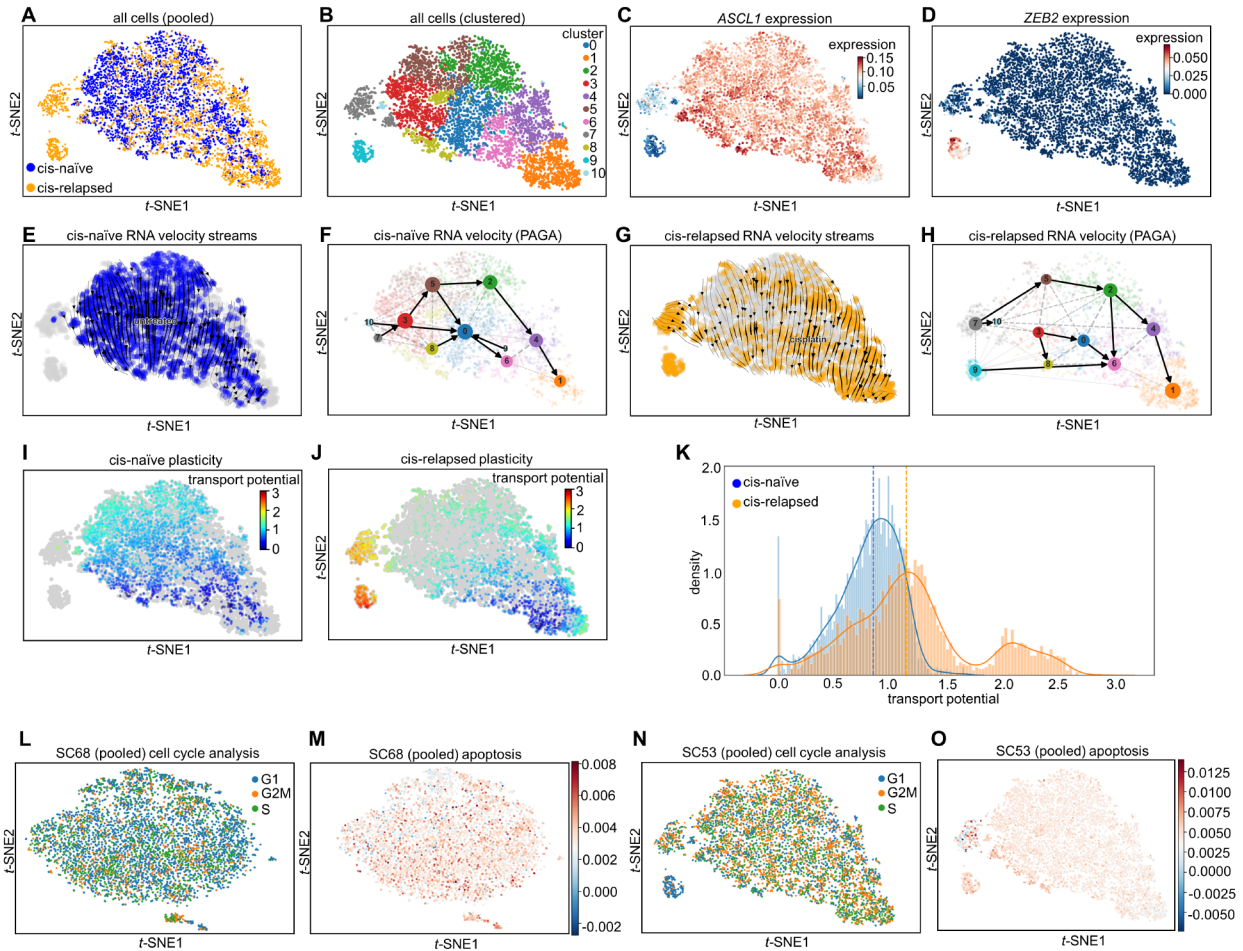


Gene Expression Detected

● NO
 ● YES



Supplementary Figure 8, related to Figure 6: Emergence of SCLC-I populations coincides with cisplatin resistance in SCLC-A predominant xenograft models. t-SNE feature plots from scRNAseq for *HES1*, *DLL3*, and *MYC* comparing parental, treatment-naïve and cisplatin-resistant/relapsed (cis-relapsed) CDX models (MDA-SC53, **A**, **C**, **E**; MDA-SC68, **B**, **D**, **F**). Violin plots comparing *ASCL1* expression between MDA-SC53 treatment-naïve and cisplatin-relapsed xenograft tumors in all cells (**G**) and only *ASCL1*-positive cells (**H**), as well as EMT score for *ASCL1*-positive cells only for both MDA-SC68 (**I**) and MDA-SC53 (**J**). Sample sizes: n=2000 cells (**A-J**). *p*-values were calculated using two-sided T-test (**H-J**).



Supplementary Figure 9, related to Figure 7: Emerging SCLC-I populations support tumor-wide resistance via transcriptional plasticity. tSNE projection of all cells from MDA-SC53 CDXs with treatment history (A) or Leiden clustering assignment (B) denoted. Expression of *ASCL1* (C) and *ZEB2* (D) in these cells. RNA velocity vector streams and PAGA maps for cells from cisplatin-naïve (E-F) and cisplatin-relapsed (G-H) CDX tumors. Cell plasticity, as measured by cell transport potential, for cells from cisplatin-naïve (I) and cisplatin-relapsed (J) tumors highlighting areas of greatest plasticity appear within island cluster within relapsed tumor. Comparison of transport potential between cisplatin-naïve and -relapsed cells (K) demonstrating higher overall plasticity in cisplatin-relapsed cells. Expression of cell cycle-specific and apoptosis-specific gene lists in pooled cells from MDA-SC68 (L-M) and MDA-SC53 (N-O). Sample sizes: n=4000 cells total (pooled) (A-O).

Supplementary Table 2, related to Figure 1: Frequency and intensity of ASCL1/NEUROD1/POU2F3 expression in human SCLC tumors.

Tumor ID	% Nuclei ASCL1+	ASCL1 H-score	% Nuclei NEUROD1+	NEUROD1 H-score	% Nuclei POU2F3+	POU2F3 H-score
1	42.55	67.25	82.66	199.14	17.85	48.02
2	72.74	154.98	7.70	12.02	8.32	23.93
3	86.20	187.78	0.13	0.24	0.04	1.04
4	76.08	154.33	43.49	96.47	1.34	3.52
5	72.64	176.55	32.79	80.23	0.54	1.55
6	2.68	2.89	0.55	1.41	57.57	150.87
7	12.16	12.66	0.21	0.40	0.52	1.49
8	82.63	183.79	53.66	107.01	1.02	2.92
9	71.26	116.52	9.21	21.71	0.96	2.74
10	36.26	42.90	87.19	226.72	1.49	4.18
11	5.50	5.58	0.05	0.10	85.64	229.74
12	90.67	187.39	1.07	1.18	2.72	7.61
13	67.06	99.76	12.08	19.06	0.86	2.44
14	58.22	119.07	34.83	59.82	0.99	2.87

Supplementary Table 3, related to Figure 5: Single-cell expression of ASCL1/NEUROD1/POU2F3 in patient-derived SCLC xenografts.

Model	A-N-P-	A-N-P+	A-N+P-	A-N+P+	A+N-P-	A+N-P+	A+N+P-	A+N+P+
Frontline								
MDA-SC4	3.85%	0	0	0	95.80%	0	0.35%	0
MDA-SC39	1.60%	0	0	0	88.70%	0	9.70%	0
MDA-SC53	7.20%	0	0.40%	0	92.00%	0.10%	0.30%	0
MDA-SC68	1.15%	0	0	0	98.85%	0	0	0
MDA-SC75	5.60%	0	0	0	93.95%	0	0.45%	0
Relapsed								
MDA-SC16	6.95%	0	0	0	88.25%	0	4.65%	0
MDA-SC49	9.90%	0	89.45%	0	0	0	0.55%	0
MDA-SC53rel	17.10%	0	0.85%	0	80.80%	0.10%	1.20%	0
MDA-SC55	6.45%	0	0.65%	0	89.30%	0.65%	2.95%	0
MDA-SC68rel	10.00%	0	0	0	89.45%	0	0.55%	0